



**HAL**  
open science

## Functional impact of Aurora A-mediated phosphorylation of HP1gamma at serine 83 during cell cycle progression.

Adrienne Grzenda, Phoebe Leonard, Seungmae Seo, Angela Mathison, Guillermo Urrutia, Ezequiel Calvo, Juan Iovanna, Raul Urrutia, Gwen Lomberk

### ► To cite this version:

Adrienne Grzenda, Phoebe Leonard, Seungmae Seo, Angela Mathison, Guillermo Urrutia, et al.. Functional impact of Aurora A-mediated phosphorylation of HP1gamma at serine 83 during cell cycle progression.. *Epigenetics and Chromatin*, 2013, 6 (1), pp.21. 10.1186/1756-8935-6-21. inserm-00843064

**HAL Id: inserm-00843064**

**<https://inserm.hal.science/inserm-00843064>**

Submitted on 10 Jul 2013

**HAL** is a multi-disciplinary open access archive for the deposit and dissemination of scientific research documents, whether they are published or not. The documents may come from teaching and research institutions in France or abroad, or from public or private research centers.

L'archive ouverte pluridisciplinaire **HAL**, est destinée au dépôt et à la diffusion de documents scientifiques de niveau recherche, publiés ou non, émanant des établissements d'enseignement et de recherche français ou étrangers, des laboratoires publics ou privés.

RESEARCH

Open Access

# Functional impact of Aurora A-mediated phosphorylation of HP1 $\gamma$ at serine 83 during cell cycle progression

Adrienne Grzenda<sup>1</sup>, Phoebe Leonard<sup>2</sup>, Seungmae Seo<sup>1</sup>, Angela J Mathison<sup>1</sup>, Guillermo Urrutia<sup>1</sup>, Ezequiel Calvo<sup>3</sup>, Juan Iovanna<sup>4</sup>, Raul Urrutia<sup>1,5</sup> and Gwen Lomber<sup>1,2,5\*</sup>

## Abstract

**Background:** Previous elegant studies performed in the fission yeast *Schizosaccharomyces pombe* have identified a requirement for heterochromatin protein 1 (HP1) for spindle pole formation and appropriate cell division. In mammalian cells, HP1 $\gamma$  has been implicated in both somatic and germ cell proliferation. High levels of HP1 $\gamma$  protein associate with enhanced cell proliferation and oncogenesis, while its genetic inactivation results in meiotic and mitotic failure. However, the regulation of HP1 $\gamma$  by kinases, critical for supporting mitotic progression, remains to be fully characterized.

**Results:** We report for the first time that during mitotic cell division, HP1 $\gamma$  colocalizes and is phosphorylated at serine 83 (Ser<sup>83</sup>) in G<sub>2</sub>/M phase by Aurora A. Since Aurora A regulates both cell proliferation and mitotic aberrations, we evaluated the role of HP1 $\gamma$  in the regulation of these phenomena using siRNA-mediated knockdown, as well as phosphomimetic and nonphosphorylatable site-directed mutants. We found that genetic downregulation of HP1 $\gamma$ , which decreases the levels of phosphorylation of HP1 $\gamma$  at Ser<sup>83</sup> (P-Ser<sup>83</sup>-HP1 $\gamma$ ), results in mitotic aberrations that can be rescued by reintroducing wild type HP1 $\gamma$ , but not the nonphosphorylatable S83A-HP1 $\gamma$  mutant. In addition, proliferation assays showed that the phosphomimetic S83D-HP1 $\gamma$  increases 5-ethynyl-2'-deoxyuridine (EdU) incorporation, whereas the nonphosphorylatable S83A-HP1 $\gamma$  mutant abrogates this effect. Genome-wide expression profiling revealed that the effects of these mutants on mitotic functions are congruently reflected in G<sub>2</sub>/M gene expression networks in a manner that mimics the on and off states for P-Ser<sup>83</sup>-HP1 $\gamma$ .

**Conclusions:** This is the first description of a mitotic Aurora A-HP1 $\gamma$  pathway, whose integrity is necessary for the execution of proper somatic cell division, providing insight into specific types of posttranslational modifications that associate to distinct functional outcomes of this important chromatin protein.

**Keywords:** Heterochromatin protein 1 (HP1), Mitosis, Aurora kinase, Epigenetics, Spindle pole, Centrosome

## Background

Heterochromatin protein 1 (HP1), the reader of histone H3 lysine 9 methylation (H3K9me), was originally discovered through studies in *Drosophila melanogaster* of mosaic gene silencing, known as position effect variegation [1,2]. In human and other mammalian cells, the

three mammalian HP1 isoforms, HP1 $\alpha$ , HP1 $\beta$  and HP1 $\gamma$ , have been well-studied for their localization, as well as their roles within the heterochromatic regions that associate with gene silencing. However, subsequent investigations have made it increasingly unmistakable that HP1 proteins not only localize to heterochromatic regions but also euchromatic regions [3,4]. These proteins are involved in diverse cellular processes, ranging from chromatin modification and epigenetic gene silencing to replication and DNA repair to nuclear architecture and chromosomal stability [3,4]. Moreover, HP1 proteins respond to a diversity of signaling pathways and acquire

\* Correspondence: lomberg.gwen@mayo.edu

<sup>1</sup>Laboratory of Epigenetics and Chromatin Dynamics, GIH Division, Department of Medicine, Biochemistry and Molecular Biology, Guggenheim 10, Mayo Clinic, 200 First Street SW, Rochester, MN 55905, USA

<sup>2</sup>Department of Obstetrics and Gynecology, Guggenheim 10, Mayo Clinic, 200 First Street SW, Rochester, MN 55905, USA

Full list of author information is available at the end of the article

various posttranslational modifications, which impact on their function [5-9]. We have previously reported that, during interphase, phosphorylation of HP1 $\gamma$  at serine 83 (P-Ser<sup>83</sup>-HP1 $\gamma$ ) via the cAMP-protein kinase A (PKA) pathway upon activation of cell surface receptors relocates this protein to euchromatin, where it plays a role in transcriptional elongation [8]. Thus, it is essential to define HP1-mediated pathways to map useful networks of membrane-to-chromatin signaling cascades for better understanding of the regulation of important cellular processes.

Ample evidence indicates that HP1 $\gamma$  is important during both somatic and germ cell proliferation. Indeed, high levels of HP1 $\gamma$  protein associate with enhanced somatic and meiotic cell proliferation [10]. Genetic inactivation of HP1 $\gamma$  results in both meiotic and mitotic failure [11,12]. Studies in primordial germ cells demonstrate that loss of HP1 $\gamma$  also reduces their cell number through impaired cell cycle progression [13]. However, the responsible molecular mechanisms that link this vital biological process to the functional regulation of HP1 $\gamma$  remain unknown.

Earlier investigations have found that HP1 $\gamma$  is phosphorylated throughout the cell cycle and, in particular, hyperphosphorylated in mitosis [14]. In the current study, we report a novel pathway, whereby HP1 $\gamma$  is regulated by mitotic kinases, in particular, Aurora kinase A, a master regulator of mitotic transitions [15]. We demonstrate that HP1 $\gamma$  is phosphorylated at serine 83 (Ser<sup>83</sup>) in G<sub>2</sub>/M where it colocalizes with Aurora A kinase, and its mitotic targets, cyclin B1, cyclin B2 and cyclin-dependent kinase 1 (CDK1) during cell division. HP1 $\gamma$  is phosphorylated at Ser<sup>83</sup> by Aurora A in vitro and in cells. In addition, siRNA-mediated knockdown of HP1 $\gamma$  leads to a decrease of P-Ser<sup>83</sup>-HP1 $\gamma$  accompanied by mitotic aberrations. Notably, reintroduction of wild type HP1 $\gamma$  rescues, to a significant extent, these abnormal mitotic effects, while the nonphosphorylatable S83A-HP1 $\gamma$  mutant is unable to rescue this consequence of HP1 $\gamma$  knockdown. Congruent with these functions, phosphomimetic S83D-HP1 $\gamma$  results in an increase of cell proliferation, whereas the nonphosphorylatable S83A-HP1 $\gamma$  mutant abrogates this effect. In addition, overexpression of either the S83A-HP1 $\gamma$  or S83D-HP1 $\gamma$  mutant supports this effect in resultant cell cycle-related gene expression networks. Thus, together, these results reveal that a novel Aurora A-HP1 $\gamma$  pathway targeting Ser<sup>83</sup> phosphorylation is necessary for the proper execution of cell division, thereby extending our knowledge of the biochemical and cell biological function of this important chromatin protein.

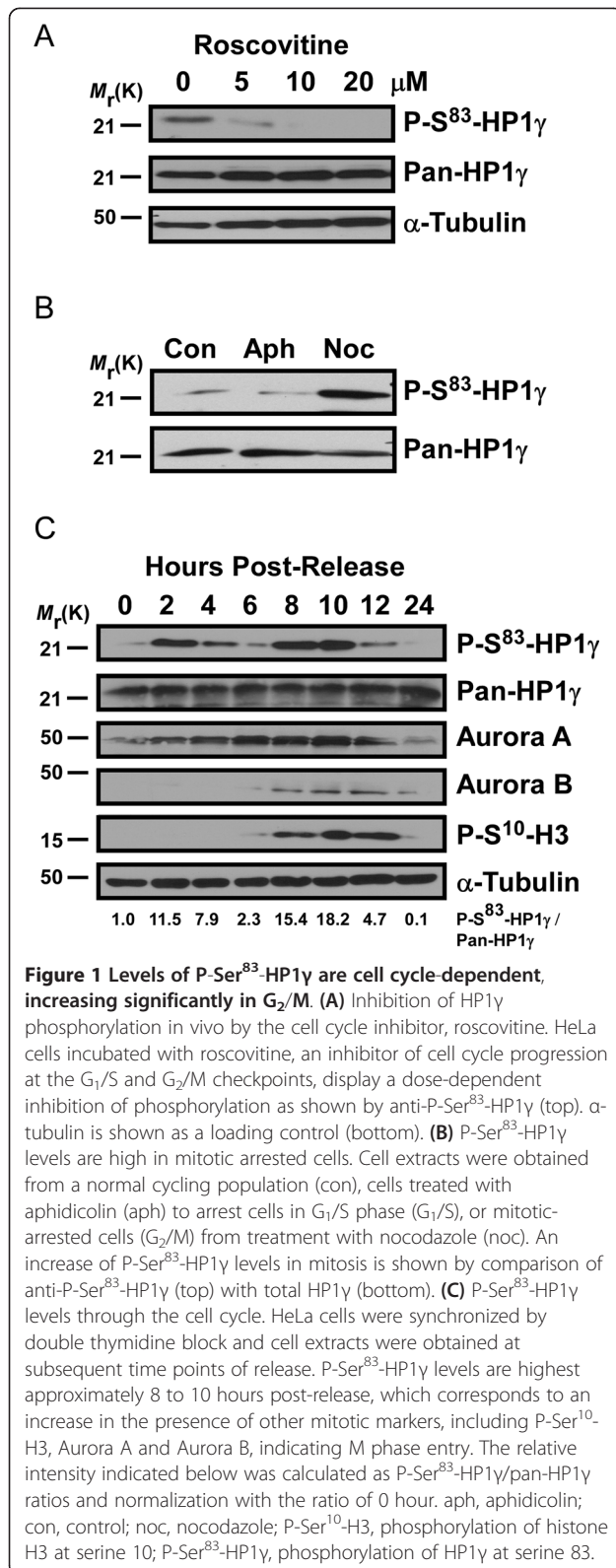
## Results

### HP1 $\gamma$ is phosphorylated at the G<sub>2</sub>/M phase of the cell cycle

We have previously described that P-Ser<sup>83</sup>-HP1 $\gamma$  by PKA mediates extracellular signals during interphase [8].

In the current study, we uncover a new Aurora kinase A-mediated pathway that phosphorylates Ser<sup>83</sup>-HP1 $\gamma$  during mitosis, which is necessary for the proper execution of this process. For this purpose, we initially analyzed the kinetics of phosphorylation in HeLa cells arrested in different phases of the cell cycle. Treatment with roscovitine, a membrane permeable cyclin-dependent kinase (CDK) inhibitor, that arrests cell cycle progression at the G<sub>1</sub>/S and G<sub>2</sub>/M checkpoints [16], resulted in dose-dependent inhibition of P-Ser<sup>83</sup>-HP1 $\gamma$  (Figure 1A). To better define the temporal pattern of these events, we treated with either aphidicolin to arrest cells in S phase, or nocodazole to obtain mitotic arrest (G<sub>2</sub>/M). The mitotic population demonstrated a striking increase in P-Ser<sup>83</sup>-HP1 $\gamma$  levels in comparison to the normal cycling population and S phase arrested cells (Figure 1B). To define these events in the absence of kinase inhibitors, we synchronized HeLa cells by double thymidine block to obtain cell extracts at subsequent time points of release from cell cycle arrest. These experiments revealed that the levels of P-Ser<sup>83</sup>-HP1 $\gamma$  peaked twice, the first at 2 hours post-release (G<sub>1</sub>/S boundary, Figure 1C, Additional file 1: Figure S1 A). As this peak was likely the phosphorylation event coinciding with the previously described involvement of PKA during interphase [8], we utilized the PKA-specific inhibitor, KT5720, to treat HeLa cells upon release from double thymidine block. Upon KT5720 treatment, P-Ser<sup>83</sup>-HP1 $\gamma$  levels at 2 hours post-release were significantly diminished (Additional file 1: Figure S1 B). However, of greater interest, a more prominent second peak across 8 to 10 hours post-release from cell cycle arrest, which coincided with G<sub>2</sub>/M, was observed (Figure 1C, Additional file 1: Figure S1A). The lower P-Ser<sup>83</sup>-HP1 $\gamma$  levels seen in-between these two peaks (4 to 6 hours post-release, Figure 1C) corresponded with S phase (Additional file 1: Figure S1A), similar to aphidicolin treatment. These results demonstrate that levels of P-Ser<sup>83</sup>-HP1 $\gamma$  peak significantly at G<sub>2</sub>/M phase during the cell cycle, suggesting that phosphorylation of this protein may play a role in cell division.

Subsequently, we sought to complement the biochemical assays of phosphorylation described above by mapping the temporal pattern of staining for P-Ser<sup>83</sup>-HP1 $\gamma$  during cell cycle progression. For this purpose, we performed immunofluorescence using confocal microscopy in cells co-stained with the anti-P-Ser<sup>83</sup>-HP1 $\gamma$  and different cell cycle markers. We utilized cyclin D as a marker of G<sub>1</sub>, 5-ethynyl-2'-deoxyuridine (EdU)-pulse labeling for S phase, and cyclin B to indicate the G<sub>2</sub> and M phases of the cell cycle. Figure 2A,B,C, which represents a low magnification field of cells stained with the anti-P-Ser<sup>83</sup>-HP1 $\gamma$ , demonstrates that the level and distribution of the signal for this modified form of HP1 $\gamma$  is variable in epithelial cells growing under normal conditions. Thus, we examined more carefully the levels and



distribution of P-Ser<sup>83</sup>-HP1 $\gamma$  signals in relationship to key cell cycle markers. P-Ser<sup>83</sup>-HP1 $\gamma$  localization in cyclin D-positive cells (G<sub>1</sub>) appeared in the euchromatic compartment of the nucleus as a fine punctate pattern (Figure 2D,E,F). Quantification of cyclin D-positive cells demonstrated that 76.6% of this population (160/209) had P-Ser<sup>83</sup>-HP1 $\gamma$  staining. However, staining was relatively negligible in cells that were positively marked by a short pulse of EdU, indicative of S phase (Figure 2G,H,I) with only 22.7% of EdU-positive cells (34/150) having any P-Ser<sup>83</sup>-HP1 $\gamma$  signal. The strongest P-Ser<sup>83</sup>-HP1 $\gamma$  signal was found in 88.3% of cyclin B-positive cells (182/206), which corresponded to G<sub>2</sub> (Figure 2J,K,L), and the signal continued through M in prometaphase, metaphase and anaphase, until returning to similar levels as G<sub>1</sub> during telophase and cytokinesis (Figure 2M,N,O,P,Q,R). Thus, these results were congruent with our biochemical studies and confirmed that P-Ser<sup>83</sup>-HP1 $\gamma$  occurs as two peaks, beginning at G<sub>1</sub> and ending at S, and the second peak which begins at G<sub>2</sub> and continues during M. Interestingly, a conspicuous feature of P-Ser<sup>83</sup>-HP1 $\gamma$  localization was its staining in cyclin B-positive cells for which the nuclear membrane has not yet disassembled (late G<sub>2</sub> prophase), in which the P-Ser<sup>83</sup>-HP1 $\gamma$  punctate pattern was stronger and present not only in euchromatin but also within centrosomes (Figure 2L). Although the cyclin B-positive cells found in M demonstrated reduced P-Ser<sup>83</sup>-HP1 $\gamma$  signal on chromosomes, a strong signal continued to localize at the centrosome region of the mitotic spindle (Figure 2M,N,O,P). In all these cases, P-Ser<sup>83</sup>-HP1 $\gamma$  coincided with the presence of cyclin B at the centrosome. As several mitotic kinases are highly enriched at this organelle [17], these studies prompted us to identify the kinase responsible for the significant P-Ser<sup>83</sup>-HP1 $\gamma$  event found during mitotic progression.

#### HP1 $\gamma$ is phosphorylated at G<sub>2</sub>/M by Aurora A

While PKA was implicated in the first peak of P-Ser<sup>83</sup>-HP1 $\gamma$  levels that occur at G<sub>1</sub>, the kinase that mediates the second peak of P-Ser<sup>83</sup>-HP1 $\gamma$  at G<sub>2</sub>/M, described here, remained unknown. Interestingly, we found that the temporal pattern of P-Ser<sup>83</sup>-HP1 $\gamma$  coincided with phosphorylation of histone H3 at serine 10 (P-Ser<sup>10</sup>-H3, Figure 1C). P-Ser<sup>10</sup>-H3 initiates during G<sub>2</sub> in pericentric foci and spreads along the chromosome arms, thus serving as a hallmark of mitosis [18]. Previously derived consensus sequences for Aurora kinases suggested that, similar to P-Ser<sup>10</sup>-H3, Ser<sup>83</sup>-HP1 $\gamma$  might be a target of Aurora kinases [19]. Additional experiments demonstrated that the temporal pattern of P-Ser<sup>83</sup>-HP1 $\gamma$  was similar to both Aurora A and Aurora B (Figure 1C). These results led us to hypothesize that the newly described P-Ser<sup>83</sup>-HP1 $\gamma$  at G<sub>2</sub>/M was achieved through the

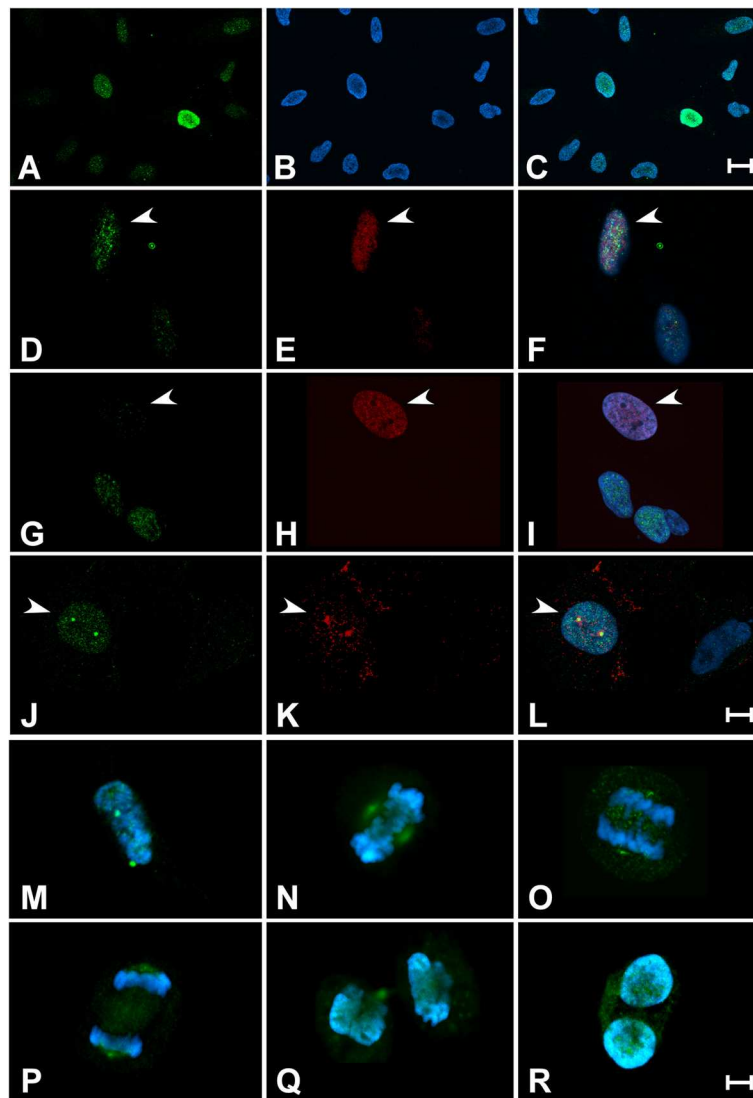


**Figure 2 Biphasic P-Ser<sup>83</sup>-HP1 $\gamma$  is observed during cell cycle progression.** (A,B,C) P-Ser<sup>83</sup>-HP1 $\gamma$  levels vary during the cell cycle. Panoramic view of a growing population of HeLa cells staining with anti-P-Ser<sup>83</sup>-HP1 $\gamma$  (A, green) demonstrates that the signal for this protein varies in intensity in different cells. Cells were counterstained with DAPI (B, blue) to show DNA and overlay is shown in (C). Three main populations are observed according to the strength of the signal, namely strong, moderate and negligible. Scale bar represents 20  $\mu$ M. (D,E,F) P-Ser<sup>83</sup>-HP1 $\gamma$  displays punctate euchromatic localization in G<sub>1</sub> phase. Localization of P-Ser<sup>83</sup>-HP1 $\gamma$  (D, green) was determined in cyclin D-positive cells (E, red), indicative of G<sub>1</sub> phase, as shown with arrows and in overlay (F). (G,H,I) Levels of P-Ser<sup>83</sup>-HP1 $\gamma$  diminish during S phase. Negligible P-Ser<sup>83</sup>-HP1 $\gamma$  signal (G, green) is found in the majority of cells undergoing S phase (arrows), as determined by EdU positively labeled cells (H, red). Overlay is shown in (I). (J,K,L) P-Ser<sup>83</sup>-HP1 $\gamma$  levels increase upon G<sub>2</sub> entry. Cyclin B-positive cells (K, red), before nuclear envelope breakdown (G<sub>2</sub>), not only shows the P-Ser<sup>83</sup>-HP1 $\gamma$  signal (J, green) as a strong punctate pattern in euchromatin, but also with separating centrosomes (L, overlay). Scale bar represents 10  $\mu$ M for panels (D to L). (M,N,O,P,Q,R) P-Ser<sup>83</sup>-HP1 $\gamma$  levels persist through mitosis. Cyclin B-positive, prometaphase cell demonstrates an increase in P-Ser<sup>83</sup>-HP1 $\gamma$  in association with separating centrosomes (M). Metaphase cell shows the P-Ser<sup>83</sup>-HP1 $\gamma$  remains localized to centrosomes, which are forming the mitotic spindle (N). Early (O) and late (P) anaphase, as well as telophase (Q) cells are shown, where the P-Ser<sup>83</sup>-HP1 $\gamma$  signal intensity at the centrosomes is decreased as cells prepare to complete cell division. P-Ser<sup>83</sup>-HP1 $\gamma$  signal within euchromatic regions is again observed during cytokinesis (R). Scale bar represents 5  $\mu$ M for panels (M to R). DAPI, 4',6-diamidino-2-phenylindole; EdU, 5-ethynyl-2'-deoxyuridine; P-Ser<sup>83</sup>-HP1 $\gamma$ , phosphorylation of HP1 $\gamma$  at serine 83.

activity of an Aurora kinase. Thus, we first performed immunofluorescence experiments to determine whether P-Ser<sup>83</sup>-HP1 $\gamma$  co-localized with any of these kinases at G<sub>2</sub>/M. Indeed, we found that P-Ser<sup>83</sup>-HP1 $\gamma$  localized to areas rich in Aurora A (Figure 3A,B,C), but not Aurora B

(Figure 3D,E,F). P-Ser<sup>83</sup>-HP1 $\gamma$  was also confirmed to be present at the Aurora A-rich area of the spindle poles through colocalization with  $\gamma$ -tubulin (Figure 3G,H,I) and  $\alpha$ -tubulin (Figure 3J,K,L). More importantly, we found that critical regulators of G<sub>2</sub>/M progression, which are

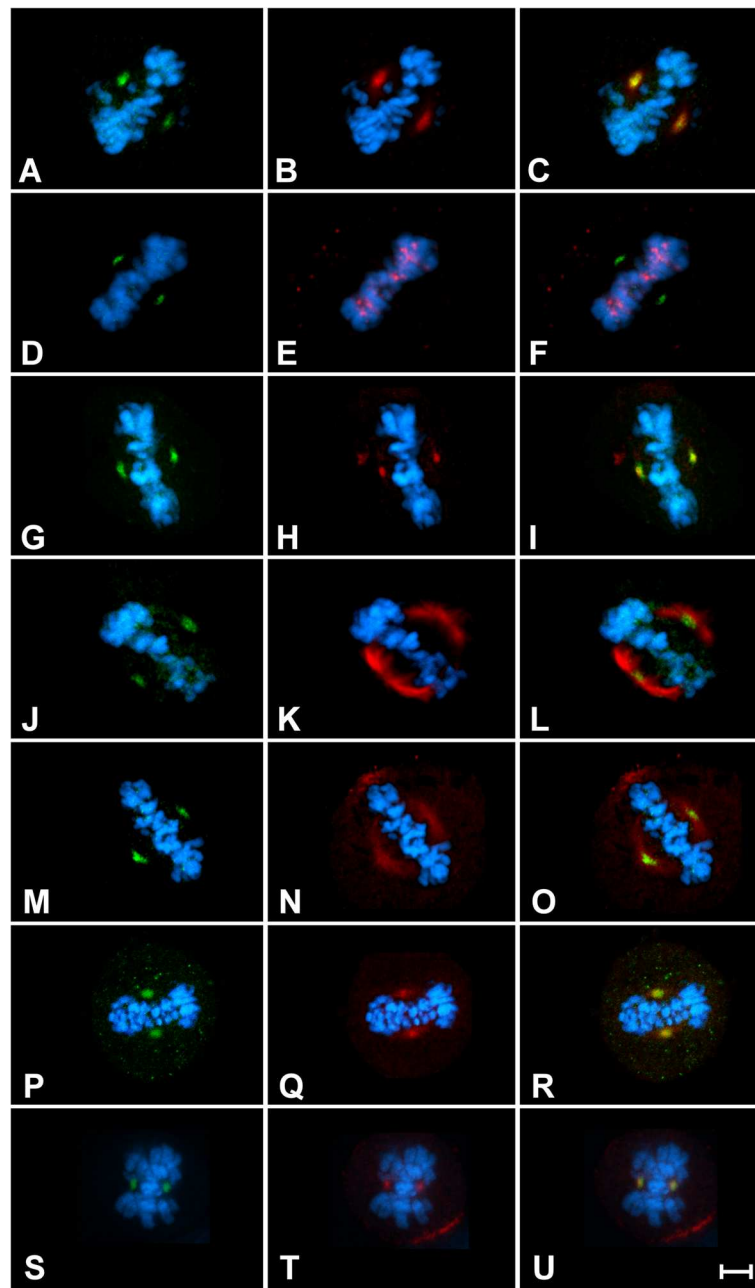


**Figure 3** P-Ser<sup>83</sup>-HP1 $\gamma$  colocalizes with Aurora A at the mitotic spindle. Representative images are shown for localization in mitotic HeLa cells. (A,B,C) Colocalization of P-Ser<sup>83</sup>-HP1 $\gamma$  (A, green) is shown with Aurora A (B, red) at the spindle poles. The overlay is shown in (C). (D,E,F) Cells in metaphase were also stained for P-Ser<sup>83</sup>-HP1 $\gamma$  (D, green) and Aurora B (E, red), which demonstrates that there is no colocalization of these two proteins as observed in the overlay (F). (G,H,I,J,K,L) P-Ser<sup>83</sup>-HP1 $\gamma$  (G,J, green) was confirmed to be present at the spindle poles through co-staining with  $\gamma$ -tubulin (H, red) as well as  $\alpha$ -tubulin (K, red) as shown in the overlays (I, L). (M,N,O,P,Q,R,S,T,U) In addition, CDK1 (N, red), cyclin B1 (Q, red) and cyclin B2 (T, red) were each shown to co-localize with P-Ser<sup>83</sup>-HP1 $\gamma$  (M,P,S, green) as shown by overlays (O,R,U). Cells were counterstained with DAPI (blue) to show DNA. Scale bar represents 5  $\mu$ M. CDK1, cyclin-dependent kinase 1; DAPI, 4',6-diamidino-2-phenylindole; P-Ser<sup>83</sup>-HP1 $\gamma$ , phosphorylation of HP1 $\gamma$  at serine 83.

also targets of Aurora A, namely cyclin B1, cyclin B2 and their partner kinase, CDK1, also colocalized with P-Ser<sup>83</sup>-HP1 $\gamma$  (Figure 3M,N,O,P,Q,U). Together, these results demonstrated that mitotic phosphorylation confers a distinct localization of this HP1 $\gamma$  subpopulation to the

spindle poles that is marked by the G<sub>2</sub>/M Aurora A-cyclin B-CDK1 pathway, supporting the idea that this kinase may be the enzyme involved in P-Ser<sup>83</sup>-HP1 $\gamma$  at G<sub>2</sub>/M.

To mechanistically test this hypothesis, we initially incubated glutathione S-transferase (GST) fusion wild type

and nonphosphorylatable mutant HP1 $\gamma$  proteins with each Aurora kinase, Aurora A or Aurora B, followed by western blot using the phospho-specific P-Ser<sup>83</sup>-HP1 $\gamma$  antibody. These in vitro kinase assays demonstrated that the wild type HP1 $\gamma$ , but not the dominant negative, nonphosphorylatable S83A-HP1 $\gamma$  mutant [8], could be phosphorylated in vitro by both Aurora A and Aurora B (Figure 4A). To determine whether Aurora kinases also

phosphorylate HP1 $\gamma$  in vivo, we performed western blots of siRNA-treated HeLa cells against Aurora A and B, separately (Figure 4B). We found that Aurora A siRNA can inhibit the P-Ser<sup>83</sup>-HP1 $\gamma$  in vivo, whereas Aurora B siRNA demonstrated only a slight reduction in levels of P-Ser<sup>83</sup>-HP1 $\gamma$  (56% of control levels). Of note, Aurora A kinase depletion by siRNA also leads to arrest of cells at G<sub>2</sub>/M [20], thus eliminating the influence of the G<sub>1</sub>

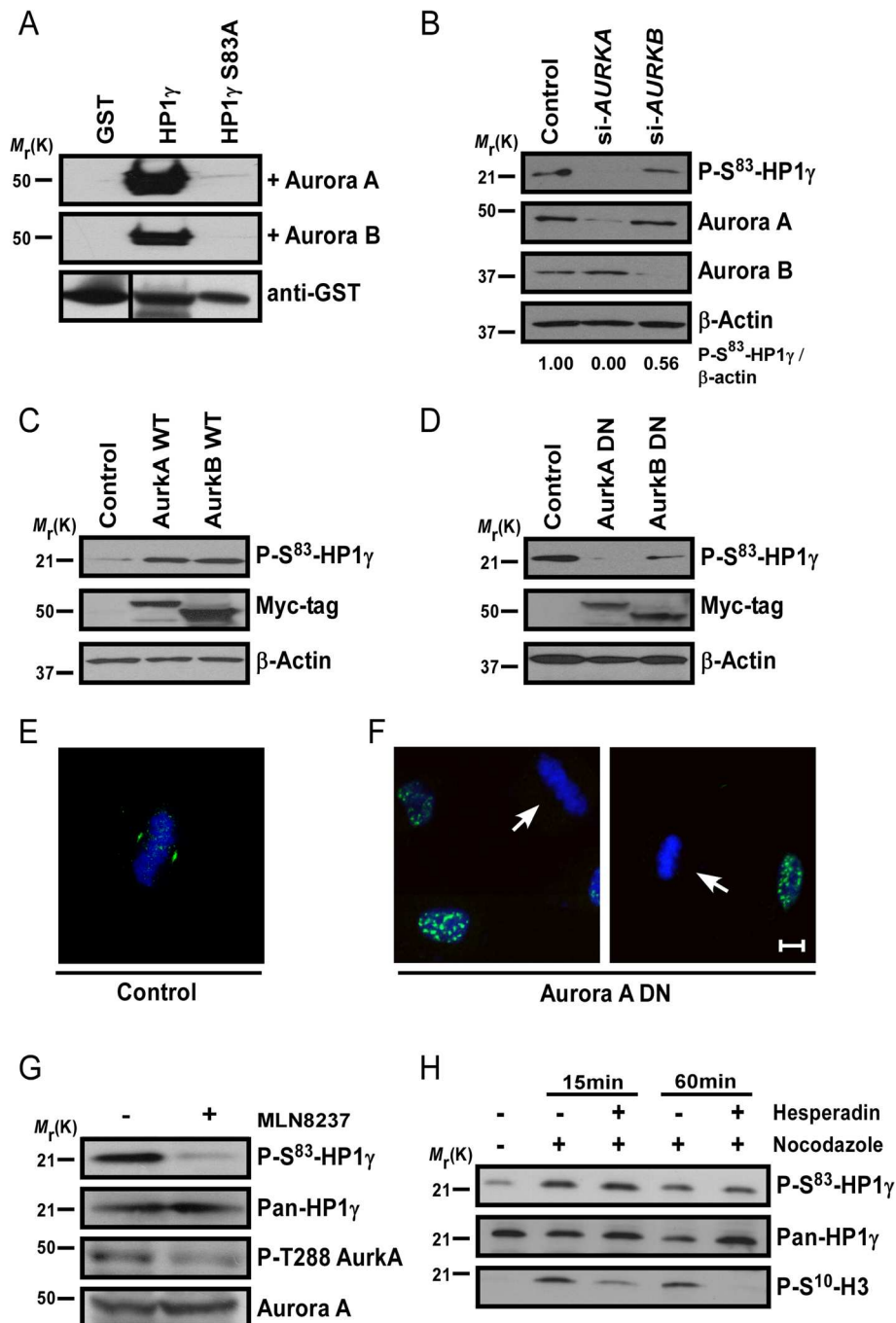


**Figure 4** (See legend on next page.)

(See figure on previous page.)

**Figure 4 Aurora A phosphorylates Ser<sup>83</sup>-HP1 $\gamma$  in G<sub>2</sub>/M. (A)** Aurora kinases phosphorylate Ser<sup>83</sup> in vitro. In vitro kinase assays were performed on GST fusion proteins, which demonstrate that wild type, not S83A-HP1 $\gamma$  mutant, is phosphorylated by Aurora kinases. **(B)** Aurora A siRNA reduces P-Ser<sup>83</sup>-HP1 $\gamma$ . Aurora A siRNA significantly reduced P-Ser<sup>83</sup>-HP1 $\gamma$ , whereas Aurora B siRNA only slightly reduced P-Ser<sup>83</sup>-HP1 $\gamma$  (top). Aurora A (*AURKA*) and Aurora B (*AURKB*) were effectively knocked-down (middle panels). Relative intensities were calculated as P-Ser<sup>83</sup>-HP1 $\gamma$ / $\beta$ -actin ratios. **(C)** Wild type Aurora kinases increase P-Ser<sup>83</sup>-HP1 $\gamma$ . CHO cells, with low basal P-Ser<sup>83</sup>-HP1 $\gamma$ , demonstrated increased P-Ser<sup>83</sup>-HP1 $\gamma$  (top) upon transfection of Aurora kinases (Myc-tag; middle). **(D)** Aurora A-dominant negative (DN) reduces P-Ser<sup>83</sup>-HP1 $\gamma$ . P-Ser<sup>83</sup>-HP1 $\gamma$  (top) was significantly reduced with Aurora A-DN in BxPC3, epithelial cells with high basal P-Ser<sup>83</sup>-HP1 $\gamma$ . Aurora B-DN also reduced P-Ser<sup>83</sup>-HP1 $\gamma$ , although still detected. Aurora-DN levels are shown by Myc-tag.  $\beta$ -actin serves as loading control (B, C, D; bottom). **(E,F)** Aurora A-DN abolishes mitotic P-Ser<sup>83</sup>-HP1 $\gamma$ . Representative images of overlays with DAPI counterstain are shown for P-Ser<sup>83</sup>-HP1 $\gamma$  (green) with control (E) or Aurora A-DN (F). Typical P-Ser<sup>83</sup>-HP1 $\gamma$  localization was still observed in interphase with Aurora A-DN, but disrupted in metaphase (arrows). Scale bar represents 10  $\mu$ m. **(G,H)** Pharmacological inhibition of Aurora A, but not Aurora B, inhibits P-Ser<sup>83</sup>-HP1 $\gamma$ . Aurora A inhibition with MLN8237 was confirmed by loss of activated P-Thr<sup>288</sup> relative to total Aurora A (G, lower panels). P-Ser<sup>83</sup>-HP1 $\gamma$  was significantly reduced with MLN8237, without affecting pan-HP1 $\gamma$  (G, upper panels). Conversely, Aurora B inhibition by hesperidin did not reduce P-Ser<sup>83</sup>-HP1 $\gamma$  (H, top). Aurora B inhibition was confirmed by P-Ser<sup>10</sup>-H3, a well-known Aurora B target (H, bottom). CHO, Chinese hamster ovary; DAPI, 4',6-diamidino-2-phenylindole; DN, dominant negative; GST, glutathione S-transferase; P-Ser<sup>10</sup>-H3, phosphorylation of histone H3 at serine 10; P-Ser<sup>83</sup>-HP1 $\gamma$ , phosphorylation of HP1 $\gamma$  at serine 83; P-Thr<sup>288</sup>, phosphorylation of Aurora A at threonine 288; Ser<sup>83</sup>, serine 83.

phosphorylation in these experiments. To further investigate the participation of Auroras in this event, Chinese hamster ovary (CHO) cells, which have relatively low basal levels of P-Ser<sup>83</sup>-HP1 $\gamma$ , were transfected with either wild type Aurora A or Aurora B (Figure 4C). As a result, levels of P-Ser<sup>83</sup>-HP1 $\gamma$  were higher in the Aurora-transfected cells than control. This occurred with both Aurora A and Aurora B transfection, as expected due to their effects on cell cycle progression. In contrast, transfection of epithelial cells, BxPC3, which have high basal levels of P-Ser<sup>83</sup>-HP1 $\gamma$ , with the dominant negative form of Aurora A [21,22] resulted in reduced levels of P-Ser<sup>83</sup>-HP1 $\gamma$  (Figure 4D). Similar to the siRNA experiments, dominant negative Aurora B [21,23] had less effect on P-Ser<sup>83</sup>-HP1 $\gamma$  levels than Aurora A. Therefore, we utilized the dominant negative Aurora A in HeLa cells to confirm this phenomenon by immunofluorescence. Compared to control cells (Figure 4E), transfections with dominant negative Aurora A (Figure 4F) abolished the localization of the P-Ser<sup>83</sup>-HP1 $\gamma$  in cell compartments rich in this kinase (arrow). In contrast, transfection with dominant negative Aurora A did not affect P-Ser<sup>83</sup>-HP1 $\gamma$  levels or localization in interphase cells (Figure 4F). Furthermore, we utilized the Aurora A- and Aurora B-specific pharmacological inhibitors, MLN8237 and hesperidin, respectively, to determine the participation of each kinase in P-Ser<sup>83</sup>-HP1 $\gamma$ . We found that specific inhibition of Aurora A with 300 nM MLN8237, which was confirmed by loss of activated phosphorylation of Aurora A at threonine 288 (P-Thr<sup>288</sup>) [24], diminished P-Ser<sup>83</sup>-HP1 $\gamma$  levels without affecting total HP1 $\gamma$  protein levels (Figure 4G). However, treatment with hesperidin (200 nM) for specific inhibition of Aurora B did not reduce P-Ser<sup>83</sup>-HP1 $\gamma$  levels, while still inhibiting the Aurora B target P-Ser<sup>10</sup>-H3 (Figure 4H, and personal communication with H Dormann and CD Allis). Combined, these results demonstrate that Aurora A kinase is primarily responsible for the localization and increased level of P-Ser<sup>83</sup>-HP1 $\gamma$  observed in G<sub>2</sub>/M.

Together with the biochemical experiments described above, these data implicate, for the first time, Aurora kinase in the cell cycle-regulated P-Ser<sup>83</sup>-HP1 $\gamma$ . This observation also represents the first evidence describing mammalian HP1 at the spindle poles, a localization that is preferred by a large amount of proteins involved in the regulation of cell cycle transitions.

#### P-Ser<sup>83</sup>-HP1 $\gamma$ is required for normal mitotic function

Functionally, HP1 $\gamma$  has been previously shown to play a role in cell cycle progression [10-13], although how this protein is regulated to modulate this function remains unknown. Inhibition of Aurora A leads to mitotic spindle defects and misaligned chromosomes [25,26]. Thus, as phosphorylation of HP1 $\gamma$  is downstream of this pathway during mitosis, we investigated whether disrupting the function of this protein also coincides with this effect. For this purpose, we performed stable lentiviral-mediated shRNA knockdown of HP1 $\gamma$  (shHP1 $\gamma$ ) in HeLa cells. HP1 $\gamma$  knockdown was confirmed by western blot with approximately 90% reduction in protein levels (Figure 5A). These cells also displayed a significant decrease in P-Ser<sup>83</sup>-HP1 $\gamma$  staining by immunofluorescence (Figure 5B), demonstrating that localization of P-Ser<sup>83</sup>-HP1 $\gamma$  to the mitotic spindle pole was unambiguous. We found that 25.5% of shHP1 $\gamma$  cells in mitosis displayed abnormalities (n = 200, Figure 5C), including multipolar spindles, centrosome disruption or lagging, unorganized chromosomes (Figure 5D). shRNA control cells (shCTRL) displayed abnormalities in only 1% (n = 200). However, in spite of this informative outcome, since HP1 $\gamma$  knockdown depleted all forms of the protein, the contribution of Ser<sup>83</sup> phosphorylation to this effect could not be assessed by this experimental manipulation. Thus, to better determine the role that phosphorylation of Ser<sup>83</sup> plays in this function, we sought to rescue the knockdown phenotype with wild type and Ser<sup>83</sup> mutant HP1 $\gamma$ . Transduction with empty vector (EV) control did

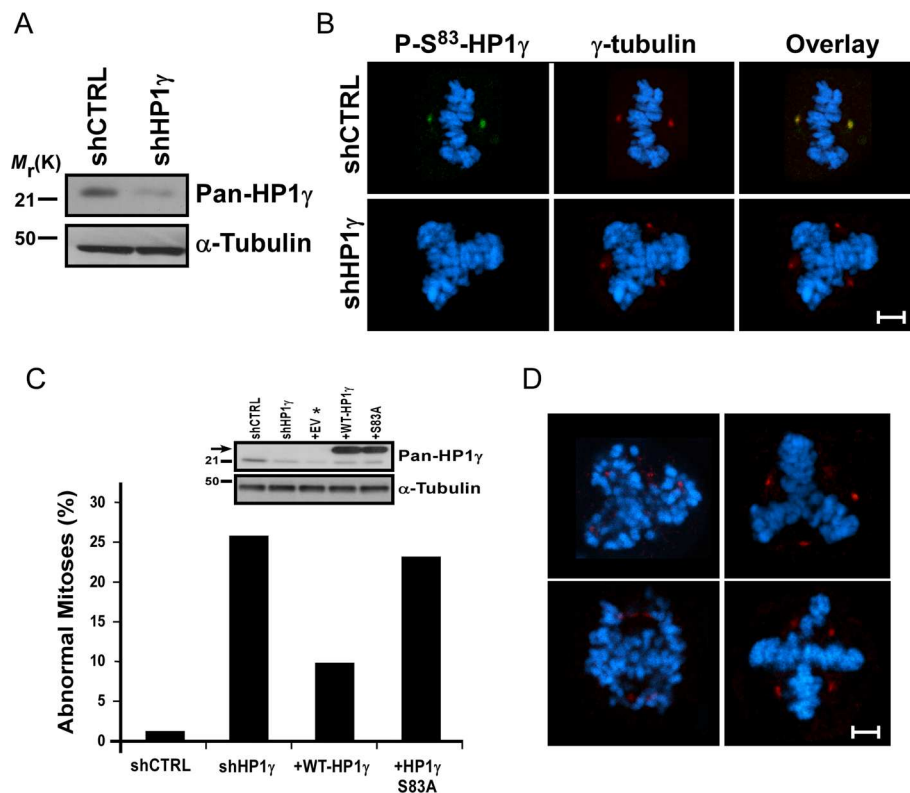


**Figure 5 P-Ser<sup>83</sup>-HP1 $\gamma$  is necessary for proper mitotic function.** (A) Stable knockdown of HP1 $\gamma$  in HeLa cells. Western blot of HP1 $\gamma$  levels (top) is shown from HeLa cell lysates to confirm stable lentiviral-mediated shHP1 $\gamma$  compared to shCTRL.  $\alpha$ -tubulin serves as a loading control (bottom). (B) HP1 $\gamma$  knockdown eliminates P-Ser<sup>83</sup>-HP1 $\gamma$  at the spindle poles. Representative images are shown for immunofluorescence on shCTRL and shHP1 $\gamma$  HeLa cells to demonstrate specific loss of P-Ser<sup>83</sup>-HP1 $\gamma$  (green) staining. Co-staining with  $\gamma$ -tubulin (red) was performed to establish the localization of the spindle poles. Cells were counterstained with DAPI and the overlay is shown. Scale bar represents 5  $\mu$ m. (C) Mitotic aberrations caused by HP1 $\gamma$  knockdown are rescued by wild type, but not S83A-HP1 $\gamma$  mutant. Mitotic aberrations were quantified for shCTRL and shHP1 $\gamma$  cells. In order to determine if Ser<sup>83</sup> phosphorylation plays a role in this function, shHP1 $\gamma$  cells were infected with adenovirus carrying wild type or S83A-HP1 $\gamma$  mutant. While reintroduction of wild type HP1 $\gamma$  was able to significantly rescue this effect, S83A-HP1 $\gamma$  mutant was not, implicating Aurora A-mediated phosphorylation in this phenomenon. For each condition, 200 mitotic cells were analyzed. Western blot is shown of endogenous HP1 $\gamma$  levels (inlay, top) as well as transduced His-tagged wild type and S83A-HP1 $\gamma$  mutant proteins (arrow).  $\alpha$ -tubulin serves as a loading control (inlay, bottom). \*Transduction with EV control did not change the number of abnormalities observed with shHP1 $\gamma$ . (D) Mitotic aberrations observed in stable shHP1 $\gamma$  cells include multipolar spindles, centrosome disruption and lagging, unorganized chromosomes. Representative images are shown for the types of observed mitotic aberrations.  $\gamma$ -tubulin (red) marks spindle poles with DAPI counterstain to show condensed mitotic chromosomes. Scale bar represents 5  $\mu$ m. DAPI, 4',6-diamidino-2-phenylindole; EV, empty vector; P-Ser<sup>83</sup>-HP1 $\gamma$ , phosphorylation of HP1 $\gamma$  at serine 83; Ser<sup>83</sup>, serine 83; shCTRL, shRNA control; shHP1 $\gamma$ , shRNA knockdown of HP1 $\gamma$ ; shRNA, short hairpin RNA.

not change the number of abnormalities observed with shHP1 $\gamma$ . Reintroduction of wild type HP1 $\gamma$  (+WT-HP1 $\gamma$ ) rescued, to a significant extent, the abnormal mitotic effects seen with knockdown of this protein (10% abnormal, n = 200). Notably, an alanine substitution, which rendered HP1 $\gamma$  unable to undergo phosphorylation at Ser<sup>83</sup> (+S83A), was unable to rescue the knockdown phenotype (23% abnormal, n = 200). This data indicates that first, normal HP1 $\gamma$  levels are necessary for proper mitotic functions and second, HP1 $\gamma$  must be amenable to Aurora A-mediated Ser<sup>83</sup> phosphorylation to achieve these effects.

#### P-Ser<sup>83</sup>-HP1 $\gamma$ status affects cell proliferation and mitotic gene expression networks

Normal mitotic cell division is a prerequisite for proliferative homeostasis and proper cell cycle progression [27]. Thus, based on our results demonstrating the role of P-Ser<sup>83</sup>-HP1 $\gamma$  in mitosis, we examined the resultant effects of P-Ser<sup>83</sup>-HP1 $\gamma$  on cell proliferation by analyzing cells transfected with wild type, S83A-HP1 $\gamma$  or S83D-HP1 $\gamma$  mutant via EdU incorporation. We found that wild type HP1 $\gamma$  had a slight increase in EdU incorporation compared to EV control (103.9%  $\pm$  2.6% of EV control, Figure 6A). However, nonphosphorylatable S83A-HP1 $\gamma$

mutant decreased the levels of EdU ( $94.2\% \pm 1.6\%$  of EV control,  $P < 0.05$ , Figure 6A). Notably, an aspartic acid substitution (S83D), designed to mimic Ser<sup>83</sup> phosphorylation, had a significant increase in levels of EdU incorporation over control cells ( $111.2\% \pm 2.6\%$  of EV control,  $P < 0.05$ , Figure 6A). Thus, these results support the idea that phosphorylation of Ser<sup>83</sup> is necessary for the regulation of cell cycle progression by HP1 $\gamma$ .

We next investigated whether the changes observed in EdU incorporation by both phosphomimetic and

nonphosphorylatable Ser<sup>83</sup>-HP1 $\gamma$  mutants were accompanied by changes in other biochemical surrogates for cell cycle progression, such as known mitotic gene networks. For this purpose, we performed a genome-wide query using Affymetrix (Santa Clara, CA, USA) profiles as transcriptional readouts of their effects. Hierarchical clustering of targets significantly altered by HP1 $\gamma$  (526 targets), S83A-HP1 $\gamma$  (492 targets) or S83D-HP1 $\gamma$  (1,727 targets) overexpression demonstrated that gene networks modulated by HP1 $\gamma$  experienced deregulation in the presence of

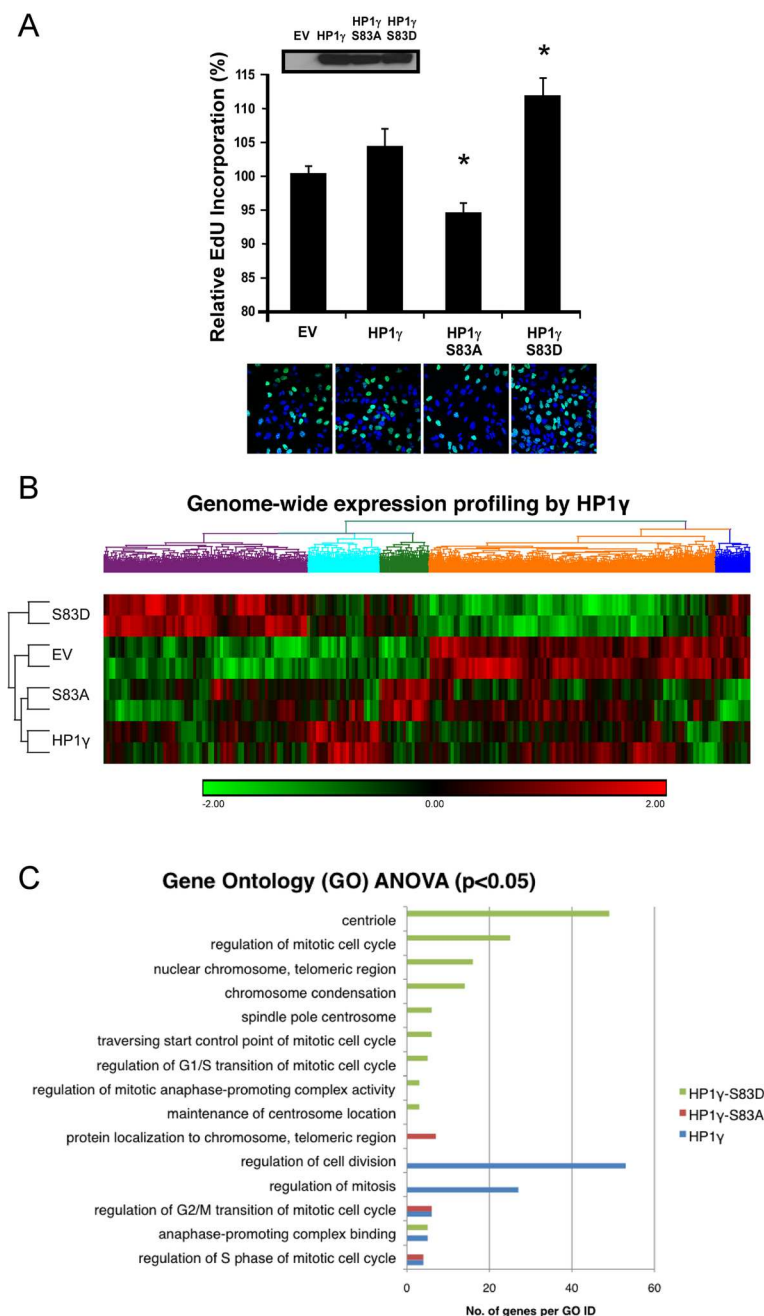


Figure 6 (See legend on next page.)

(See figure on previous page.)

**Figure 6 P-Ser<sup>83</sup>-HP1 $\gamma$  status alters cell proliferation and cell cycle-related gene networks.** (A) P-Ser<sup>83</sup>-HP1 $\gamma$  plays a role in cell proliferation. Cell proliferation was measured in the presence of control (EV), wild type HP1 $\gamma$ , the nonphosphorylatable (S83A)- or phosphomimetic (S83D)-HP1 $\gamma$  mutants by EdU incorporation, using both FACS and microscopy. Wild type HP1 $\gamma$  demonstrated only a slight increase in EdU incorporation compared to EV. However, while mutation of S83A-HP1 $\gamma$  decreased the levels of EdU, the S83D-HP1 $\gamma$  mutant had a significant increase in levels of EdU incorporation over control cells. Western blot controlling expression of His-tagged wild type and mutant HP1 $\gamma$  proteins is shown (top, inset). A representative immunofluorescence image (40  $\times$  magnification) of EdU-positive cells (green) is shown below each respective experimental condition. Cells were counterstained with DAPI to detect total number of cells present in a field. \**P* values <0.05. (B) Genome-wide expression analysis of HP1 $\gamma$  highlights consequences of Ser<sup>83</sup> phosphorylation. Hierarchical clustering of significant targets (*P* value <0.05) from Affymetrix Human Gene 1.0 ST microarray demonstrates the close relationship between EV and the nonphosphorylatable S83A-HP1 $\gamma$  mutant. Large clusters of genes show deregulation in the presence of either the nonphosphorylatable (S83A)- or phosphomimetic (S83D)-HP1 $\gamma$  mutants. (C) P-Ser<sup>83</sup>-HP1 $\gamma$  status influences the expression of G<sub>2</sub>/M-related genes. Gene Ontology (GO) ANOVA reveals significant differential expression of genes by both wild type and mutant HP1 $\gamma$  in functional groupings related to mitosis and cell division, again indicating that the presence of an active phosphorylation site at Ser<sup>83</sup> is necessary for proper mitotic function as a sizeable number of targets are deregulated in the presence of the HP1 $\gamma$  mutants with altered phosphorylation abilities. ANOVA, analysis of variance; DAPI, 4',6-diamidino-2-phenylindole; EdU, 5-ethynyl-2'-deoxyuridine; EV, empty vector; FACS, fluorescence-activated cell sorting; GO, Gene Ontology; P-Ser<sup>83</sup>-HP1 $\gamma$ , phosphorylation of HP1 $\gamma$  at serine 83; Ser<sup>83</sup>, serine 83.

the Ser<sup>83</sup> mutation, indicating dependence of these processes on regulation of Ser<sup>83</sup> phosphorylation (Figure 6B). Based on Euclidean distance calculation and the resulting dendrogram, both control and nonphosphorylatable S83A-HP1 $\gamma$  mutant samples were statistically the most similar (Figure 6B). The fact that the EV and the S83A-HP1 $\gamma$  mutant possessed the closest relationship suggested that the latter worked predominantly as either an inactive or dominant negative mutant. However, the phosphomimetic S83D-HP1 $\gamma$  mutant, for the most part, reversed the effect of the S83A-HP1 $\gamma$  mutant, suggesting that it likely worked in a constitutively active manner thereby mimicking Aurora A-mediated Ser<sup>83</sup> phosphorylation. Pathway-specific RT-PCR was used to validate a subset of significant targets (Additional file 2: Table S1). These experiments revealed that HP1 $\gamma$  and its phosphorylated form have the ability to change the levels of transcripts related to mitosis.

Gene Ontology (GO) ANOVA analysis was utilized to probe for differentially expressed functional groupings of genes (Figure 6C). Overall, HP1 $\gamma$  overexpression resulted in significant enrichment of targets related to regulation of cellular proliferation, cell division, and mitosis (*P* <0.05). S83A-HP1 $\gamma$  mutant overexpression yielded differential expression in targets related to protein localization to the chromosome, regulation of the S phase of the mitotic cell cycle and regulation of the G<sub>2</sub>/M transition of mitotic cell cycle. S83D-HP1 $\gamma$  mutant overexpression showed significant alteration in genes related to the regulation of the mitotic cell cycle, regulation of the G<sub>2</sub>/M anaphase-promoting complex, maintenance of centrosome location and spindle pole structure, among others. Consequently, from these data, we conclude that disruption of phosphorylation status of HP1 $\gamma$  has diverse effects on multiple aspects of the mitotic cell cycle, which is congruent with its cell cycle-associated phosphorylation pattern (Figures 1 and 2) indicating a pervasive role of the regulation of HP1 $\gamma$  in cell division.

Interestingly, previous studies have shown that depletion of HP1 $\gamma$  in primordial germ cells reduces their

number as a result of impaired cell cycle progression [13]. Comparison of our expression dataset with a published dataset in primordial germ cells revealed that the expression of the nonphosphorylatable S83A-HP1 $\gamma$  mutant displayed a highly similar pattern as HP1 $\gamma$  depletion, including targets related to cell cycle, proliferation and growth. This ability of the S83A-HP1 $\gamma$  mutation to mimic conditions of absolute HP1 $\gamma$  depletion at the level of gene expression networks, combined with the inability of the S83A-HP1 $\gamma$  mutant to rescue the mitotic defects observed with HP1 $\gamma$  knockdown, indicates that posttranslational modification of this residue is needed for proper progression through mitosis. Furthermore, it may be concluded from our genome-wide analysis that HP1 $\gamma$  participates in the regulation of processes, which support proper cell division and proliferation through phosphorylation-dependent and phosphorylation-independent mechanisms.

## Discussion

Based on the current study, our demonstration that HP1 $\gamma$ , a well-known epigenetic regulator, undergoes robust phosphorylation at Ser<sup>83</sup> in G<sub>2</sub>/M has significant biological relevance and deserves careful consideration. Previous studies demonstrating that HP1 proteins are ejected from chromosomes during mitosis [28,29] led to the assumption that this protein is not involved in the regulation of this process, even though it is highly expressed in rapidly dividing cancer cells [10]. In this regard, the current study reveals that, during G<sub>2</sub>/M, an extrachromosomal subpopulation of HP1 $\gamma$ , P-Ser<sup>83</sup>-HP1 $\gamma$ , localizes with  $\gamma$ -tubulin, Aurora A kinase and other mitotic targets, including cyclin B1, cyclin B2 and CDK1, at the spindle poles. Thus, this data demonstrates for the first time that, in spite of its ejection from chromosomes, HP1 $\gamma$  does not disappear during mitosis, but rather relocates to organelles, known for enrichment in cell cycle regulators, where it undergoes G<sub>2</sub>/M-specific phosphorylation at Ser<sup>83</sup> by Aurora A. In addition, the colocalization and coupling of Aurora A to HP1 $\gamma$  in cell

cycle regulation is reconstituted in time and space in each cell cycle.

Examination of the effect of the related kinase, Aurora B, demonstrates that this enzyme can phosphorylate the Ser<sup>83</sup> site in vitro. However, siRNA and dominant negative experiments demonstrate that Aurora B was not as robust as Aurora A on modulating levels of P-Ser<sup>83</sup>-HP1 $\gamma$  in cells. Treatment of cells with the Aurora B inhibitor, hesperidin, does not impair P-Ser<sup>83</sup>-HP1 $\gamma$  and, more importantly, Aurora B does not localize with P-Ser<sup>83</sup>-HP1 $\gamma$  in mitotic cells. These results reveal a significant level of specificity for these kinases in the phosphorylation of HP1 proteins.

We found that HP1 $\gamma$ , though ejected from chromosomes by the previously described Aurora-mediated P-Ser<sup>10</sup>-H3 [28,29], remains tightly associated to a mitotic organelle which is rich in cell cycle regulators. This reveals the existence of coupled mechanisms of ejection and relocalization of HP1 $\gamma$ , which ultimately has significant consequences for the regulation of cell division. Both steps involved in this process, H3 and HP1 $\gamma$  phosphorylation, are mediated by Aurora kinases. Thus, it is most likely that one function of Auroras has evolved, in part, to secure that epigenetic regulators are turned on and off during cell division in a highly synchronized manner, to achieve the proper transfer of genetic-epigenetic material through generations. Interestingly, although HP1 proteins themselves have not been previously observed at the centrosome/spindle pole, several HP1-interacting proteins are known to reside in this cell compartment. For example, a subpopulation of origin recognition complex 2 (Orc2) protein has been localized to centrosomes [30]. However, contrary to the Aurora A-cyclin B-CDK1 pathway, which links the phosphorylation of HP1 $\gamma$  at the spindle during G<sub>2</sub>/M transition, Orc2 associates with HP1 only in the population that is tightly bound to heterochromatin in G<sub>1</sub> and early S phase. In addition, immunoprecipitation of Orc2 shows specific interaction with HP1 $\alpha$  and HP1 $\beta$ , but not HP1 $\gamma$  [30], the HP1 protein studied here. Since posttranslational modifications of HP1 were not considered in the Orc2 experiments, it remains possible that subpopulations of distinct posttranslationally modified HP1 proteins, such as P-Ser<sup>83</sup>-HP1 $\gamma$ , which cannot be detected with pan-HP1 antibodies, also interact with Orc2. It is not likely, however, that Orc2 is responsible for recruitment of HP1 $\gamma$  to this cell compartment, given that Orc2 is localized there throughout the entire cell cycle [30]. Nevertheless, our results demonstrate a high degree of selectivity for HP1 $\gamma$  to work with certain regulatory enzymes (kinases) to maintain mitotic functions.

Previous studies have shown that disruption of G9a, one of the histone methyltransferases responsible for the histone mark recognized and bound by HP1, H3 lysine

9, results in chromosome instability along with centrosome abnormalities [31]. In addition to creating the mark to which HP1 binds, G9a localizes with HP1 $\alpha$  and HP1 $\gamma$ , which is dependent upon its own automethylation [32], and HP1 $\gamma$  has been shown to specifically form complexes with G9a in the context of the E2F-6 gene silencing complex [33]. Interestingly, in meiosis cell division during gamete production, HP1 $\gamma$  and G9a are proposed to form an axis that is responsible for retaining centromeric regions of unpaired homologous chromosomes in close alignment, and facilitating progression of their pairing in early meiotic prophase [12]. In fact, HP1 $\gamma$ -deficient mouse spermatocytes undergo meiotic catastrophe [12]. An important observation of our studies is that siRNA-mediated knockdown of HP1 $\gamma$  leads to a decrease of P-Ser<sup>83</sup>-HP1 $\gamma$  accompanied by mitotic aberrations. While reintroduction of wild type HP1 $\gamma$  rescues, to a significant extent, these abnormal mitotic effects, the nonphosphorylatable S83A-HP1 $\gamma$  mutant is unable to rescue this consequence of HP1 $\gamma$  knockdown, highlighting the importance of Ser<sup>83</sup> modification for this function. Moreover, the S83D-HP1 $\gamma$  mutant that mimics Aurora A phosphorylation facilitates cell proliferation, whereas the nonphosphorylatable S83A-HP1 $\gamma$  mutant inhibits this process. Therefore, it is tempting to speculate whether modifications of HP1 influence interactions with G9a and whether these proteins function together in regulating proper cell division. Indeed, additional studies using model organisms support that the function described here for human HP1 proteins is conserved. In *Schizosaccharomyces pombe*, the HP1 homologue, Swi6, is required to preserve genomic integrity and proper segregation of chromosomes during mitosis [34]. Impaired Swi6 function leads to mitotic alterations that cause severe growth alterations. Furthermore, the HP1-like protein in *Dictyostelium discoideum*, AX4 chromo domain-containing protein (hcpA), which displays 79% similarity to human HP1 $\gamma$ , colocalizes with electron-dense structures at the nuclear periphery that are compatible with pericentrosomal material [35]. Overexpression of this protein causes growth defects that are accompanied by an increase in the frequency of atypical anaphase bridges. Genetic studies in *Drosophila* have demonstrated that mutations in the HP1 protein cause defective chromosome segregation [36,37]. Thus, in combination with this data, the studies described here indicate that HP1 proteins have evolved to support cell division in organisms ranging from fission yeast to humans.

Congruent with our results, previous experiments have defined a role for HP1 $\gamma$  in human diseases that are characterized by abnormal cell proliferation. High levels of HP1 $\gamma$  have been observed in several cancer types, including esophageal, breast, colon, lung and cervical

cancer, the cell model used here [10]. In addition, siRNA-mediated knockdown of HP1 $\gamma$  expression inhibits cervical cancer cell proliferation. Of note, Aurora A, the kinase identified in this study as responsible for P-Ser<sup>83</sup>-HP1 $\gamma$  at G<sub>2</sub>/M, is amplified and overexpressed in cervical cancer, which induces centrosome amplification, aneuploidy and transformation [38]. Cervical cancer patients with high Aurora A expression correlate with a poorer disease-free survival and overall survival rates than patients with low Aurora A expression, indicating that this protein could be used as a prognostic marker [39]. Based on the current study, the high levels of both HP1 $\gamma$  and Aurora kinases in cervical cancer cells would suggest that there is a resultant increase in P-Ser<sup>83</sup>-HP1 $\gamma$ . Thus, targeting this pathway would affect P-Ser<sup>83</sup>-HP1 $\gamma$ -mediated cell proliferation, in addition to other downstream Aurora effectors. In fact, Aurora kinase inhibitors have been shown to suppress proliferation of cervical cancer cells and enhance chemosensitivity [40,41], suggesting that targeting Aurora in combination with the HP1-histone methyltransferase pathway may be a beneficial therapy in these patients.

## Conclusions

In summary, the current study identifies a novel Aurora-HP1 $\gamma$  pathway that involves P-Ser<sup>83</sup>-HP1 $\gamma$  by Aurora A in G<sub>2</sub>/M and localization of this HP1 $\gamma$  subpopulation to the spindle pole, which is necessary for proper cell division. Combined, these results constitute robust evidence that P-Ser<sup>83</sup>-HP1 $\gamma$  plays a role in mitosis and bears importance for understanding impairments, which have been shown to be characterized by abnormally high levels of HP1 $\gamma$  and Aurora kinase activity, including cancer. Our results also suggest a teleological interpretation, namely that certain regulators of chromatin dynamics and transcription, such as HP1 $\gamma$ , may undergo functional pressures (for example Aurora A phosphorylation) to maintain the integrity of cell division so that their own epigenetic inheritance is reproducible from cell generation to cell generation.

## Methods

### Cell lines, reagents and cell treatments

Cell lines were obtained from the American Type Culture Collection (ATCC, Rockville, MD, USA) and maintained according to the manufacturer's protocol. The human LX2 cell line was obtained as a generous gift from Dr Steve Freeman (Mount Sinai, NY, USA). Roscovitine (Sigma-Aldrich, St Louis, MO, USA) treatment was added at increasing concentrations (0, 5, 10 and 20  $\mu$ M) for 8 hours, and lysates were harvested. Cells were treated with 3  $\mu$ g/ml aphidicolin or 2  $\mu$ g/ml nocodazole (both from EMD Millipore, Billerica, MA, USA) for 16 hours to arrest at G<sub>1</sub>/S and G<sub>2</sub>/M,

respectively. Control cells were treated with vehicle, dimethyl sulfoxide (DMSO). HeLa cells were synchronized by double thymidine block. Thymidine (2 mM, Sigma-Aldrich) was added to asynchronous cells for 18 hours. Cells were subsequently released for 9 hours in regular growth media prior to the second thymidine (2 mM) block. After 17 hours, cells were released for the thymidine block and lysates were collected at the indicated time points. KT5720 was obtained from EMD Millipore. MLN8237 and hesperidin were purchased from Selleckchem (Houston, TX, USA). For hesperidin treatment, HeLa cells were arrested in mitosis by treatment with nocodazole for 16 hours. Arrested cells were treated with 200 nM hesperidin for the indicated times in the presence of 10  $\mu$ M of the proteasome inhibitor MG132 (Sigma-Aldrich) to prevent mitotic exit [28].

### Plasmids, siRNA and recombinant adenovirus

Standard molecular biology techniques were used to clone HP1 $\gamma$  into the pGEX and Ad5CMV vectors. For HP1 $\gamma$ -specific transient shRNA-mediated knockdown, complementary oligonucleotides were synthesized for the target sequence (GCAAATCAAAGAAGAAAAG), annealed and ligated into the pCMS3 vector (kindly provided by Dr Daniel Billadeau, Mayo Clinic, Rochester, MN, USA). For stable shRNA-mediated HP1 $\gamma$  knockdown, control or HP1 $\gamma$ -specific shRNA lentiviral particles (Santa Cruz Biotechnology, Inc, Santa Cruz, CA, USA) were used to infect cells according to the manufacturer's protocol, followed by puromycin selection (2  $\mu$ g/ml). Myc-tagged wild type and dominant negative constructs for Aurora A and Aurora B were a kind gift from Dr Paolo Sassone-Corsi [21]. S83A-HP1 $\gamma$  and S83D-HP1 $\gamma$  mutations were obtained using the QuickChange Site-Directed Mutagenesis Kit, as suggested by the manufacturer (Agilent Technologies, Inc, Santa Clara, CA, USA). All constructs were verified by sequencing at the Molecular Biology Core at Mayo Clinic, Rochester, MN, USA. Aurora A (*AURKA*) and Aurora B (*AURKB*) Silencer validated siRNAs were purchased from Ambion-Life Technologies (Carlsbad, CA, USA). Epitope-tagged (6xHis-Xpress) HP1 $\gamma$ , S83A-HP1 $\gamma$  and S83D-HP1 $\gamma$ , as well as EV (Ad5CMV), were generated as recombinant adenovirus in collaboration with the Gene Transfer Vector Core at the University of Iowa, IA, USA.

### Western blot analysis

Samples were run on 4 to 20% gradient SDS-PAGE gels (Lonza, Walkersville, MD, USA) or 12% SDS-PAGE gels and electroblotted onto polyvinylidene difluoride (PVDF) membranes (EMD Millipore). The membranes were blocked in 5% BSA in tris-buffered saline Tween-20 (TBST) for 1 hour at room temperature. The blots were incubated for 2 hours at room temperature or overnight at 4°C with primary antibody (P-Ser<sup>83</sup>-HP1 $\gamma$  [8],

1:1,000; HP1 $\gamma$ , 1:1,000; and P-Ser<sup>10</sup>-H3, 1:5,000 (all from EMD Millipore); Aurora A, 1:1,000 (BD Biosciences Pharmingen, San Diego, CA, USA); Aurora B, 1:500; cyclin B1, 1:1,000; cyclin B2, 1:1,000; and CDK1, 1:1,000 (Abcam, Cambridge, MA, USA);  $\beta$ -actin, 1:1,000; and  $\alpha$ -tubulin, 1:1,000 (Sigma-Aldrich); c-Myc (9E10) for Myc-tagged proteins, 1:1,000 (Thermo Scientific, Rockford, IL, USA); and OMNI D8 for His-tagged proteins, 1:1,000 (Santa Cruz Biotechnology). After repeated washes in TBST, horseradish peroxidase (HRP)-conjugated anti-rabbit or mouse IgG secondary antibody (1:5,000) was added for 1 hour at room temperature. Blots were developed by Pierce ECL chemiluminescent substrate (Thermo Scientific).

#### Immunofluorescence and confocal microscopy

Immunofluorescence and confocal microscopy were performed as previously described [42]. The primary antibodies were used at the following dilutions: P-Ser<sup>83</sup>-HP1 $\gamma$ , 1:200; and  $\gamma$ -tubulin, 1:500 (Sigma-Aldrich); Aurora A, 1:50; and Aurora B, 1:50 (BD Biosciences Pharmingen); cyclin B1, 1:500; cyclin B2, 1:100; and CDK1, 1:40 (Abcam); and cyclin D3, 1:200 (Cell Signaling Technology, Danvers, MA, USA). For localization of P-Ser<sup>83</sup>-HP1 $\gamma$  during S-phase, EdU incorporation was combined with immunofluorescence. Prior to fixation, cells were incubated for 30 minutes in media containing 10  $\mu$ M EdU. Subsequently, cells were processed for immunofluorescence, followed by EdU labeling using the Click-iT EdU Imaging Assay Kit (Invitrogen, Carlsbad, CA, USA) according to the manufacturer's protocol. For mitotic aberrations, spindle poles were labeled by immunofluorescence with  $\gamma$ -tubulin and counterstained with 4',6-diamidino-2-phenylindole (DAPI) containing mounting media (Vector Laboratories, Burlingame, CA, USA). For each condition, at least 200 mitotic cells were analyzed to quantify mitotic aberrations.

#### GST fusion protein purification and in vitro kinase assays

GST fusion protein purification was done as previously described [8]. For Aurora A and Aurora B in vitro kinase assays, HP1 fusion proteins (10  $\mu$ g) were incubated with recombinant kinases (EMD Millipore) and 10 mM ATP (Sigma-Aldrich) for 10 minutes at 30°C, in either the supplied buffer (Aurora A) or buffer containing 50 mM Tris pH 7.5, 0.1 mM ethylene glycol tetraacetic acid (EGTA), and 15 mM dithiothreitol (DTT, Aurora B). Kinase reactions were terminated by the addition of SDS loading dye and then resolved by western blot as described above.

#### Cell proliferation assay

Cell proliferation was measured by EdU incorporation using both fluorescence-activated cell sorting (FACS) and microscopy. Cells were infected with adenovirus

carrying control, HP1 $\gamma$ , S83A-HP1 $\gamma$  or S83D-HP1 $\gamma$  vectors. Forty-eight hours post-plating, cells were pulsed with 10  $\mu$ M EdU (Invitrogen) for 1 hour. Subsequently, cells were processed using the Click-iT EdU Flow Cytometry or Imaging Assay Kits (Invitrogen) according to the manufacturer's protocols. EdU incorporation was measured by FACS analysis at the Mayo Flow Cytometry Research Core Facility, Rochester, MN, USA, or confocal microscopy. Each experiment was performed at least five different times in triplicate, expressed as means with standard error of mean (SEM) and statistical analyses were performed using unpaired *t*-test.

#### Gene expression profiling, microarray analysis

Global gene expression profiling was carried out at the Microarrays Facility of the Research Center of Laval University, CRCHUL, QC, Canada, utilizing the Affymetrix Human Gene 1.0 ST arrays (28,869 well-annotated genes and 764,885 distinct probes). Intensity files were generated by Affymetrix GCS 3000 7G and the GeneChip Operating Software (Affymetrix, Santa Clara, CA, USA). Data analysis, background subtraction and intensity normalization was performed using robust multi-array analysis (RMA) [43]. Genes that were differentially expressed along with false discovery rate were estimated from *t*-test ( $>0.005$ ) and corrected using Bayesian approach [44,45]. Data analysis, hierarchical clustering and ontology were performed with the oneChannelGUI to extend affyGUI graphical interface capabilities [46], and Partek Genomics Suite, version 6.5 (Partek Inc, St Louis, MO, USA) with ANOVA analysis. Final fold changes were calculated as  $x = 2^{\log_2 \text{value}}$ . Probes with *P* value  $<0.05$  and fold change  $\pm 2.2$  among HP1 $\gamma$  versus EV, S83A-HP1 $\gamma$  versus EV, and S83D-HP1 $\gamma$  versus EV were selected for further analysis. For GO ANOVA, a minimum threshold of three genes and  $P < 0.05$  was used to identify significant functional groups. To validate the Affymetrix microarray, targets with significant alteration ( $P < 0.05$ ) were compared to the real-time data using an arbitrary cutoff of  $\pm 2.2$  fold change compared to EV control.

#### Additional files

**Additional file 1: Figure S1.** (A) FACS-assisted cell cycle analysis of double thymidine block samples. HeLa cells were synchronized by double thymidine block and released for the indicated time points. Enrichment of cells is shown at the G<sub>1</sub>/S boundary 2 hours post-release, in S phase at 5 hours post-release and in mitosis at 8 hours post-release. (B) G<sub>1</sub>/S boundary peak of P-Ser<sup>83</sup>-HP1 $\gamma$  levels at 2 hours post-release from double thymidine block are diminished with PKA inhibition. PKA was inhibited with increasing concentrations of KT5720 as indicated upon release from double thymidine block and cell lysates were collected at 2 hours post-release. Pan-HP1 $\gamma$  levels are shown as a loading control. FACS, fluorescence-activated cell sorting; PKA, protein kinase A; P-Ser<sup>83</sup>-HP1 $\gamma$ , phosphorylation of HP1 $\gamma$  at serine 83.

**Additional file 2: Table S1.** q-PCR array validation of Affymetrix Human Gene 1.0 ST microarray.

### Abbreviations

ANOVA: analysis of variance; aph: aphidicolin; ATCC: American Type Culture Collection; BSA: bovine serum albumin; CDK: cyclin-dependent kinase; CDK1: cyclin-dependent kinase 1; CHO: Chinese hamster ovary; con: control; CRCHUL: Centre de Recherche du Centre Hospitalier de l'Université Laval; DAPI: 4',6-diamidino-2-phenylindole; DMSO: dimethyl sulfoxide; DTT: dithiothreitol; EdU: 5-ethynyl-2'-deoxyuridine; EGTA: ethylene glycol tetraacetic acid; EV: empty vector; FACS: fluorescence-activated cell sorting; GO: Gene Ontology; GST: glutathione S-transferase; GUI: graphical user interface; H3K9me: histone H3 lysine 9 methylation; HcpA: *Dictyostelium discoideum*, AX4 chromo domain-containing protein; HP1: heterochromatin protein 1; HRP: horseradish peroxidase; noc: nocodazole; Orc2: origin recognition complex subunit 2; PKA: protein kinase A; P-Ser<sup>10</sup>: H3: phosphorylation of histone H3 at serine 10; P-Ser<sup>83</sup>: HP1γ: phosphorylation of HP1γ at serine 83; P-Thr<sup>288</sup>: phosphorylation of Aurora A at threonine 288; PVDF: polyvinylidene difluoride; RMA: robust multi-array analysis; RT-PCR: reverse transcriptase polymerase chain reaction; SEM: standard error of mean; Ser<sup>10</sup>: serine 10; Ser<sup>83</sup>: serine 83; shCTRL: shRNA control; shHP1γ: shRNA knockdown of HP1γ; shRNA: short hairpin RNA; siRNA: small interfering RNA; TBST: tris-buffered saline Tween-20.

### Competing interests

The authors declare that they have no competing interests.

### Authors' contributions

RU and GL generated the main idea of the work and developed the study design, both conceptually and methodologically. AG, PL, SS, AJM, GU, EC and GL made substantial contributions to the acquisition of data. AG, PL, EC, JI, RU and GL contributed to analysis and interpretation of data. AG, RU and GL wrote the manuscript from first draft to completion. AG, PL, SS, AJM, GU, EC, JI, RU and GL made comments, suggested appropriate modifications and corrections. All authors read and approved the final manuscript.

### Acknowledgements

This work was supported by funding from the Fraternal Order of Eagles and a Career Development Award from the Mayo Clinic SPORE in Pancreatic Cancer (P50 CA102701, both to GL), as well as the National Institutes of Health (grant DK52913 to RU and T32CA148073 to AG), the Mayo Clinic Center for Cell Signaling in Gastroenterology (P30DK084567), and the Mayo Foundation. The authors would like to sincerely thank Dr Debora Bensi for technical assistance during the early development of this work, as well as Holger Dormann and Dr C David Allis for their generous contributions and helpful insights for the hesperidin P-Ser<sup>83</sup>-HP1γ experiments.

### Author details

<sup>1</sup>Laboratory of Epigenetics and Chromatin Dynamics, GIH Division, Department of Medicine, Biochemistry and Molecular Biology, Guggenheim 10, Mayo Clinic, 200 First Street SW, Rochester, MN 55905, USA. <sup>2</sup>Department of Obstetrics and Gynecology, Guggenheim 10, Mayo Clinic, 200 First Street SW, Rochester, MN 55905, USA. <sup>3</sup>Molecular Endocrinology and Oncology Research Center, Centre Hospitalier de l'Université Laval (CHUL) Research Center, Quebec, QC G1V 4G2, Canada. <sup>4</sup>Institut National de la Santé et de la Recherche Médicale (INSERM), Unité 624, Stress Cellulaire, 163 Avenue de Luminy, Case 915, Parc Scientifique et Technologique de Luminy, 13288, Marseille Cedex 9, France. <sup>5</sup>Translational Epigenomics Program, Center for Individualized Medicine, Rochester, MN 55905, USA.

Received: 14 February 2013 Accepted: 14 June 2013

Published: 5 July 2013

### References

1. Eissenberg JC, James TC, Foster-Hartnett DM, Hartnett T, Ngan V, Elgin SC: **Mutation in a heterochromatin-specific chromosomal protein is associated with suppression of position-effect variegation in *Drosophila melanogaster*.** *Proc Natl Acad Sci U S A* 1990, **87**:9923–9927.

2. James TC, Elgin SC: **Identification of a nonhistone chromosomal protein associated with heterochromatin in *Drosophila melanogaster* and its gene.** *Mol Cell Biol* 1986, **6**:3862–3872.
3. Lomberk G, Wallrath L, Urrutia R: **The Heterochromatin Protein 1 family.** *Genome Biol* 2006, **7**:228.
4. Kwon SH, Workman JL: **The heterochromatin protein 1 (HP1) family: put away a bias toward HP1.** *Mol Cells* 2008, **26**:217–227.
5. Ayoub N, Jayasekharan AD, Bernal JA, Venkitaraman AR: **HP1-beta mobilization promotes chromatin changes that initiate the DNA damage response.** *Nature* 2008, **453**:682–686.
6. Martin C, Chen S, Heilos D, Sauer G, Hunt J, Shaw AG, Sims PFG, Jackson DA, Lovric J: **Changed genome heterochromatinization upon prolonged activation of the Raf/ERK signaling pathway.** *PLoS One* 2010, **5**:e13322.
7. Zhao T, Heyduk T, Eissenberg JC: **Phosphorylation site mutations in heterochromatin protein 1 (HP1) reduce or eliminate silencing activity.** *J Biol Chem* 2001, **276**:9512–9518.
8. Lomberk G, Bensi D, Fernandez-Zapico M, Urrutia R: **Evidence for the existence of an HP1-mediated subcode within the histone code.** *Nat Cell Biol* 2006, **8**:407–415.
9. Maison C, Romeo K, Bailly D, Dubarry M, Quivy JP, Almouzni G: **The SUMO protease SENP7 is a critical component to ensure HP1 enrichment at pericentric heterochromatin.** *Nat Struct Mol Biol* 2012, **19**:458–460.
10. Takanashi M, Oikawa K, Fujita K, Kudo M, Kinoshita M, Kuroda M: **Heterochromatin protein 1 gamma epigenetically regulates cell differentiation and exhibits potential as a therapeutic target for various types of cancers.** *Am J Pathol* 2009, **174**:309–316.
11. Serrano A, Rodriguez-Corsino M, Losada A: **Heterochromatin protein 1 (HP1) proteins do not drive pericentromeric cohesin enrichment in human cells.** *PLoS One* 2009, **4**:e5118.
12. Takada Y, Naruse C, Costa Y, Shirakawa T, Tachibana M, Sharif J, Kezuka-Shiotani F, Kakiuchi D, Masumoto H, Shinkai Y, Ohho K, Peters AH, Turner JM, Asano M, Koseki H: **HP1gamma links histone methylation marks to meiotic synapsis in mice.** *Development* 2011, **138**:4207–4217.
13. Abe K, Naruse C, Kato T, Nishiuchi T, Saitou M, Asano M: **Loss of heterochromatin protein 1 gamma reduces the number of primordial germ cells via impaired cell-cycle progression in mice.** *Biol Reprod* 2011, **85**:1013–1024.
14. Minc E, Allory Y, Worman HJ, Courvalin J-C, Buendia B: **Localization and phosphorylation of HP1 proteins during the cell cycle in mammalian cells.** *Chromosoma* 1999, **108**:220–234.
15. Carmena M, Earnshaw WC: **The cellular geography of Aurora kinases.** *Nat Rev Mol Cell Biol* 2003, **4**:842–854.
16. Meijer L, Borgne A, Mulner O, Chong JPY, Blow JJ, Inagaki N, Inagaki M, Delcros JG, Moulinoux JP: **Biochemical and cellular effects of roscovitine, a potent and selective inhibitor of the cyclin-dependent kinases cdc2, cdk2 and cdk5.** *Eur J Biochem* 1997, **243**:527–536.
17. Nigg EA: **Mitotic kinases as regulators of cell division and its checkpoints.** *Nat Rev Mol Cell Biol* 2001, **2**:21–32.
18. Hendzel MJ, Wei Y, Mancini MA, Van Hooser A, Ranalli T, Brinkley BR, Bazett-Jones DP, Allis CD: **Mitosis-specific phosphorylation of histone H3 initiates primarily within pericentromeric heterochromatin during G2 and spreads in an ordered fashion coincident with mitotic chromosome condensation.** *Chromosoma* 1997, **106**:348–360.
19. Sardon T, Pache RA, Stein A, Molina H, Vernos I, Aloy P: **Uncovering new substrates for Aurora A kinase.** *EMBO Rep* 2010, **11**:977–984.
20. Du J, Hannon GJ: **Suppression of p160ROCK bypasses cell cycle arrest after Aurora-A/STK15 depletion.** *Proc Natl Acad Sci U S A* 2004, **101**:8975–8980.
21. Crosio C, Fimia GM, Loury R, Kimura M, Okano Y, Zhou H, Sen S, Allis CD, Sassone-Corsi P: **Mitotic phosphorylation of histone H3: spatio-temporal regulation by mammalian Aurora kinases.** *Mol Cell Biol* 2002, **22**:874–885.
22. Li Z, Rana TM: **A kinase inhibitor screen identifies small-molecule enhancers of reprogramming and iPS cell generation.** *Nat Commun* 2012, **3**:1085.
23. Murata-Hori M, Wang YL: **The kinase activity of aurora B is required for kinetochore-microtubule interactions during mitosis.** *Curr Biol* 2002, **12**:894–899.
24. Gorgun G, Calabrese E, Hideshima T, Ecsedy J, Perrone G, Mani M, Ikeda H, Bianchi G, Hu Y, Cirstea D, Santo L, Tai YT, Nahar S, Zheng M, Bandi M, Carrasco RD, Raje N, Munshi N, Richardson P, Anderson KC: **A novel Aurora-A kinase inhibitor MLN8237 induces cytotoxicity and cell-cycle arrest in multiple myeloma.** *Blood* 2010, **115**:5202–5213.
25. Asteriti I, Giubettini M, Lavia P, Guarguaglini G: **Aurora-A inactivation causes mitotic spindle pole fragmentation by unbalancing microtubule-generated forces.** *Mol Cancer* 2011, **10**:131.

26. Hoar K, Chakravarty A, Rabino C, Wysong D, Bowman D, Roy N, Ecsedy J: **MLN8054, a small-molecule inhibitor of Aurora A, causes spindle pole and chromosome congression defects leading to aneuploidy.** *Mol Cell Biol* 2007, **27**:4513–4525.
27. Gough NR: **Focus issue: choreographing the dance of the mitotic kinases.** *Sci Signal* 2011, **4**:eg5.
28. Fischle W, Tseng BS, Dormann HL, Ueberheide BM, Garcia BA, Shabanowitz J, Hunt DF, Funabiki H, Allis CD: **Regulation of HP1-chromatin binding by histone H3 methylation and phosphorylation.** *Nature* 2005, **438**:1116–1122.
29. Hirota T, Lipp JJ, Toh BH, Peters JM: **Histone H3 serine10 phosphorylation by Aurora B causes HP1 dissociation from heterochromatin.** *Nature* 2005, **438**:1176–1180.
30. Prasanth SG, Prasanth KV, Siddiqui K, Spector DL, Stillman B: **Human Orc2 localizes to centrosomes, centromeres and heterochromatin during chromosome inheritance.** *EMBO J* 2004, **23**:2651–2663.
31. Kondo Y, Shen L, Ahmed S, Boumber Y, Sekido Y, Haddad BR, Issa JP: **Downregulation of histone H3 lysine 9 methyltransferase G9a induces centrosome disruption and chromosome instability in cancer cells.** *PLoS One* 2008, **3**:e2037.
32. Chin HG, Esteve P-O, Pradhan M, Benner J, Patnaik D, Carey MF, Pradhan S: **Automethylation of G9a and its implication in wider substrate specificity and HP1 binding.** *Nucleic Acids Res* 2007, **35**:7313–7323.
33. Ogawa H, Ishiguro K, Gaubatz S, Livingston DM, Nakatani Y: **A complex with chromatin modifiers that occupies E2F- and Myc-responsive genes in G0 Cells.** *Science* 2002, **296**:1132–1136.
34. Nonaka N, Kitajima T, Yokobayashi S, Xiao G, Yamamoto M, Grewal SIS, Watanabe Y: **Recruitment of cohesin to heterochromatic regions by Swi6/HP1 in fission yeast.** *Nat Cell Biol* 2002, **4**:89–93.
35. Kaller M, Euteneuer U, Nellen W: **Differential effects of heterochromatin protein 1 isoforms on mitotic chromosome distribution and growth in Dictyostelium discoideum.** *Eukaryot Cell* 2006, **5**:530–543.
36. Fanti L, Giovino G, Berloco M, Pimpinelli S: **The heterochromatin protein 1 prevents telomere fusions in Drosophila.** *Mol Cell* 1998, **2**:527–538.
37. Kellum R, Alberts BM: **Heterochromatin protein 1 is required for correct chromosome segregation in Drosophila embryos.** *J Cell Sci* 1995, **108**:1419–1431.
38. Zhou H, Kuang J, Zhong L, Kuo WL, Gray JW, Sahin A, Brinkley B, Sen S: **Tumour amplified kinase STK15/BTAK induces centrosome amplification, aneuploidy and transformation.** *Nat Genet* 1998, **20**:189–193.
39. Zhang W, Wang J, Liu SJ, Hua W, Xin XY: **Correlation between Aurora-A expression and the prognosis of cervical carcinoma patients.** *Acta Obstet Gynecol Scand* 2009, **88**:521–527.
40. Cheung CH, Lin WH, Hsu JT, Hour TC, Yeh TK, Ko S, Lien TW, Coumar MS, Liu JF, Lai WY, Shiao HY, Lee TR, Hsieh HP, Chang JY: **BPR1K653, a novel Aurora kinase inhibitor, exhibits potent anti-proliferative activity in MDR1 (P-gp170)-mediated multidrug-resistant cancer cells.** *PLoS One* 2011, **6**:e23485.
41. Zhang L, Zhang S: **ZM447439, the Aurora kinase B inhibitor, suppresses the growth of cervical cancer SiHa cells and enhances the chemosensitivity to cisplatin.** *J Obstet Gynaecol Res* 2011, **37**:591–600.
42. Gebelein B, Urrutia R: **Sequence-specific transcriptional repression by KS1, a multiple-zinc-finger-Kruppel-associated box protein.** *Mol Cell Biol* 2001, **21**:928–939.
43. Irizarry RA, Hobbs B, Collin F, Beazer-Barclay YD, Antonellis KJ, Scherf U, Speed TP: **Exploration, normalization, and summaries of high density oligonucleotide array probe level data.** *Biostatistics* 2003, **4**:249–264.
44. Benjamini Y, Drai D, Elmer G, Kafkafi N, Golani I: **Controlling the false discovery rate in behavior genetics research.** *Behav Brain Res* 2001, **125**:279–284.
45. Smyth GK: **Linear models and empirical bayes methods for assessing differential expression in microarray experiments.** *Stat Appl Genet Mol Biol*: Stat Appl Genet Mol Biol; 2004:3. Article3.
46. Wettenhall JM, Simpson KM, Satterley K, Smyth GK: **affyLmGUI: a graphical user interface for linear modeling of single channel microarray data.** *Bioinformatics* 2006, **22**:897–899.

doi:10.1186/1756-8935-6-21

**Cite this article as:** Grzenda et al.: Functional impact of Aurora A-mediated phosphorylation of HP1 $\gamma$  at serine 83 during cell cycle progression. *Epigenetics & Chromatin* 2013 **6**:21.

**Submit your next manuscript to BioMed Central and take full advantage of:**

- **Convenient online submission**
- **Thorough peer review**
- **No space constraints or color figure charges**
- **Immediate publication on acceptance**
- **Inclusion in PubMed, CAS, Scopus and Google Scholar**
- **Research which is freely available for redistribution**

Submit your manuscript at  
www.biomedcentral.com/submit

